Research Article

Buoyancy-surface tension driven forces on electro-thermal-convection in a rotating dielectric fluid-saturated porous layer: effect of cubic temperature gradients

B. Arpitha Raju[1] · Rudranna Nandihalli[2] · C. E. Nanjundappa[3] · I. S. Shivakumara[4]

Abstract

This paper analyses the onset of buoyancy-surface tension driven forces on rotating electro-thermal-convection in a dielectric fluid-saturated porous layer under the influence of different basic temperature gradients. The lower surface is rigid-isothermal, and the upper surface is stress-free and flat at which the Robin-type of thermal boundary condition is invoked. The principle of exchange of stability is valid and the stability eigenvalue problem is solved numerically using the Galerkin method. The parameters influencing the stability characteristics of the system are the thermal Rayleigh number (R_t), electric Rayleigh number (R_e), Marangoni number (Ma), Taylor number (Ta), Darcy number (Da), Biot number (Bi) and the viscosity ratio (Λ). The onset of convection is delayed for a nonlinear temperature profile when compared to the linear temperature profile. It is observed that the strength of surface tension force and an AC electric field is to hasten the onset. The system is found to be more stable with increasing Bi, Ta and Λ as well as decrease in Da. The surface tension and electric forces complement each other and always observed to be $Ma_c < R_{ec}$.

1 Introduction

Electrohydrodynamics (EHD) is a phenomenon which occurs in several areas of engineering ranging from aircraft and space vehicles to micro-fluidic devices [1]. One practical application of using an electric field is to pump liquids in micro-channels since it will not persuade mechanical noises. When an external electric field is applied across a fluid layer, the Maxwell stress could instigate flow instability in the liquid layer with spatial changes in electrical properties. In earlier studies, the instability of flow in the design of engineering devices is basically considered to

be triggered by an electric field due to abrupt changes [2, 3]. Of late, two intangible designs have been found with applications in the laptops cooling systems [4] and tools on a flight in space [5].

Thermal convective instability problems are studied in the presence of a uniform vertical electric field, called electro-thermal-convection (ETC). This mode of ETC has been studied by Taylor [6]. Turnbull and Melcher [7] described moderately simple laboratory-type experiments which can be expected to model the essential features of ETC to validate the theoretical prediction. Roberts [8] treated this problem in the presence of temperature gradients and

✉ B. Arpitha Raju, rajuarpitha@gmail.com; Rudranna Nandihalli, rudranna@rvce.edu.in; C. E. Nanjundappa, nanjundappace@gmail.com; I. S. Shivakumara, shivakumarais@gmail.com | ¹Department of Electrical and Electronics Engineering, Dr. Ambedkar Institute of Technology, Bengaluru 560056, India. ²Department of Electrical and Electronics Engineering, RV College of Engineering, Bengaluru 560059, India. ³Department of Mathematics, Dr. Ambedkar Institute of Technology, Bengaluru 560056, India. ⁴Department of Mathematics, Bangalore University, Bengaluru 560001, India.

electric potential differences across the fluid layer. Turnbull [9] carried out theoretical investigations on dielectrophoretic force effect on ETC, and subsequently many researchers [10–31] reviewed some related experimental and theoretical studies. Shivakumara et al. [32] studied ETC in a rotating dielectric fluid layer under a uniform vertical AC electric field. Of late, Ashwini et al. [33] investigated theoretically the effect of boundary conditions on penetrative ETC due to internal heating in a dielectric fluid-saturated porous layer. The abundant literature on this topic is available in the book by Nield and Bejan [34].

If the upper surface of the fluid layer is open to the atmosphere then the instability may also arise due to surface tension driven force, known as Marangoni convection. The convective instability may also be due to both buoyancy and surface tension forces called Bénard–Marangoni convection and studied extensively in an incompressible fluid layer (see [35, 36] and references therein). Char and Chiang [37] treated Bénard-Marangoni problem in AC electric field regime. Douiebe et al. [38] carried out theoretical investigations on Bénard-Marangoni ETC in the presence

of rotation. Hennenberg et al. [39] was the first to discuss theoretically in detail the buoyancy-surface tension driven convection in a wetting liquid saturated porous medium, while Rudraiah [40] studied on the effect of Brinkman boundary layer on the onset of electroconvection in a porous medium giving an insight to the manufactures of smart materials.

The effect of Joule heating caused by passing AC electric field through electrolyte may cause non-uniform temperature distribution. The present paper deals with theoretical aspects of the problem of Bénard-Marangoni ETC in a rotating dielectric fluid-saturated porous layer. Moreover, the study of non-uniform basic temperature gradients on the onset is interesting as it paves the way to understand control of convective instability. The following different types of non-dimensional basic temperature gradients, $f(z)$ namely,

1. Linear temperature profile (model 1): $f(z) = 1$
2. Cubic 1 temperature profile (model 2): $f(z) = 3(z - 1)^2$
3. Cubic 2 temperature profile (model 3): $f(z) = 0.66 + 1.02 (z - 1)^2$

are considered in the discussion. The eigenvalue problem is solved numerically using the Galerkin method over a large range of governing physical parameters. The model

2 offers more stabilizing effect on the system and the system is found to be least stable for model 1.

2 Governing equations

A dielectric fluid-saturated horizontal porous layer of depth d in the presence of gravity acting vertically downward in the presence of a uniform vertical AC electric field is considered as presented in Fig. 1. The porous layer is rotating about the vertical axis with a constant angular velocity $\vec{\Omega} = (0, 0, \Omega)$. The rigid lower boundary $z = 0$ and the upper stress-free non-deformable boundary $z = d$ are maintained at constant temperatures $T = T_0$ and $T = T_1$, respectively. At the upper free surface, surface tension force acts which varies linearly with temperature in the form $\sigma_m = \sigma_0 - \sigma_T(T - T_0)$, where $\sigma_T = -\partial \sigma_m / \partial T$.

The basic equations under the Oberbeck-Boussinesq approximation are (see [8, 17, 19, 37])

$$\nabla \cdot \vec{q} = 0 \tag{1}$$

$$\rho_0 \left[\frac{1}{\varphi} \frac{\partial \vec{q}}{\partial t} + \frac{1}{\varphi^2} (\vec{q} \cdot \nabla) \vec{q} \right] = -\nabla P + \rho \vec{g} + \tilde{\mu}_f \nabla^2 \vec{q} - \frac{\mu_f}{k_1} \vec{q} - \frac{2}{\varphi} (\Omega \hat{k} \times \vec{q}) - \frac{1}{2} (\vec{E}.\vec{E}) \nabla \varepsilon \tag{2}$$

$$A \frac{\partial T}{\partial t} + (\vec{q} \cdot \nabla) T = \kappa \nabla^2 T \tag{3}$$

$$\nabla \cdot \left(\varepsilon \vec{E} \right) = 0, \ \nabla \times \vec{E} = 0 \ \text{or} \ \vec{E} = -\nabla \phi \tag{4a, b}$$

$$\rho = \rho_0 \left[1 - \alpha (T - T_0) \right] \tag{5}$$

$$\varepsilon = \varepsilon_0 \left[1 - \eta (T - T_0) \right] (\alpha, \eta > 0) \tag{6}$$

where $\vec{q} = (u, v, w)$ is the velocity, T is the temperature, $\vec{E} = (E_x, E_y, E_z)$ is the electric field, φ is the porosity of the porous medium, ϕ is the electric potential, α is the thermal expansion coefficient, $\vec{g}$ is the gravitational acceleration, k_1
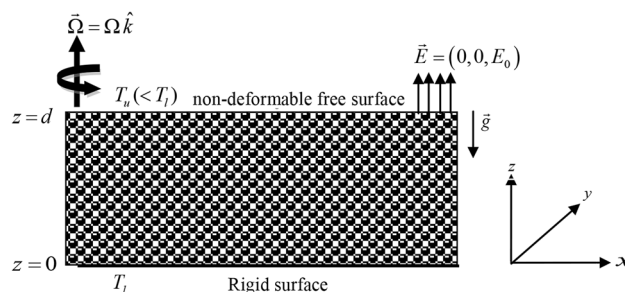

Fig. 1 Physical configuration

is the permeability of the porous medium, ε is the dielectric constant, κ is the thermal diffusivity, α is the thermal expansion coefficient, η is the dielectric constant expansion coefficient, μ_f is the fluid viscosity, $\tilde{\mu}_f$ is the effective viscosity, A is the ratio of heat capacities, ρ_0 and ε_0 are the reference density and dielectric constant, respectively at $T = T_0$.

The basic state is quiescent and taken as

$$\left[\vec{q},\, T,\, p,\, \rho,\, \vec{E},\, \varepsilon\right] = \left[0,\, T_b(z,t),\, p_b(z),\, \rho_b(z),\, \vec{E}_b(z),\, \varepsilon_b(z)\right] \tag{7}$$

In the basic state, we have

$$\frac{1}{\rho_0}\frac{dp_b}{dz} - \frac{\rho_b}{\rho_0}g + \frac{E_b^2}{2}\frac{d\varepsilon_b}{dz} = 0 \tag{8}$$

$$A\frac{\partial T_b}{\partial t} = \kappa\frac{\partial^2 T_b}{\partial z^2} \tag{9}$$

$$\nabla \cdot \left(\varepsilon_b \vec{E}_b\right) = 0. \tag{10}$$

As propounded by Nield [41], it is also not our intention to treat here the full problem of temperature profiles depending explicitly on time. Instead, we introduce a simplification in the form of a quasi-static approximation

which consists of freezing the basic temperature distribution $T_b(z,t)$ at a given instant of time. This simplification is justified so long as the disturbances are growing faster than the basic profile is evolving (Nield and Bejan [34]). Under the circumstances, the basic state temperature distribution admits a solution of the form

$$-\frac{dT_b}{dz} = f(z) \tag{11}$$

where $f(z)$ is the basic temperature gradient such that

$$\int_0^d f(z)\,dz = \Delta T/d. \tag{12}$$

On solving Eq. (10), we get

$$\varepsilon_b E_{bz} = \varepsilon_0 E_0 = \text{constant (say)}, \tag{13}$$

where

$$E_{bz} = \frac{E_0}{1 + \eta\Delta T\, z/d}. \tag{14}$$

In the basic state Eq. 4(b) yields

$$\phi_b = \frac{-E_0 d}{\eta\Delta T}\log(1 + \eta\Delta T\, z/d)$$

where $E_0 = \frac{-\phi_1\eta\Delta T/d}{\log(1+\eta\Delta T)}$ is the externally imposed AC electric field at $z = d$.

3 Linear instability analysis

To study the instability of the system, the dependent variables are perturbed over their equilibrium counterparts in the form

$$\left[\vec{q},\, p,\, \vec{E},\, T,\, \rho,\, \varepsilon\right] = \left[\vec{q}',\, p_b + p',\, E_b + \vec{E}',\, T_b + T',\, \rho_b + \rho',\, \varepsilon_b + \varepsilon'\right] \tag{15}$$

where the primed quantities are the perturbed ones and considered to be very small in comparison with the basic state quantities. Substituting Eq. (15) into Eqs. (2)–(4), using the basic state solution, linearizing the equations, eliminating the pressure from the momentum equation by operating curl twice and retaining the vertical component lead finally to arrive at the following governing stability equations

$$\left[\frac{1}{\varphi}\frac{\partial}{\partial t} - \frac{\tilde{\mu}_f}{\rho_0}\nabla^2 + \frac{\mu_f}{\kappa\rho_0}\right]\nabla^2 w = \alpha g\nabla_h^2 T - \frac{2\Omega}{\varphi}\frac{\partial\xi}{\partial z} + \varepsilon_0 E_0 \eta f(z)\left[\nabla_h^2\left(\frac{\partial\phi}{\partial z}\right) + E_0\eta\nabla_h^2 T\right] \tag{16}$$

$$\left[A\frac{\partial}{\partial t} - \kappa\nabla^2\right]T = f(z)w \tag{17}$$

$$\nabla^2\chi = -\eta E_0\frac{\partial T}{\partial z} \tag{18}$$

$$\frac{1}{\varphi}\frac{\partial\xi}{\partial t} - \frac{\tilde{\mu}_f}{\rho_0}\nabla^2\xi = \frac{2\Omega}{\varphi}\frac{\partial w}{\partial z} - \frac{\mu_f}{\kappa\rho_0}\xi \tag{19}$$

where $\xi = \partial v/\partial x - \partial u/\partial y$ is the z-component of vorticity vector and $\nabla_h^2 = \partial^2/\partial x^2 + \partial^2/\partial y^2$.

The lower boundary is rigid-isothermal, while the upper boundary is stress-free at which the surface tension force acts is non-deformable and a Robin-type of thermal boundary condition is invoked. Hence, the relevant

boundary conditions on velocity and temperature are [39, 40, 42, 43]:

$$w = \frac{\partial w}{\partial z} = 0, \quad T = 0, \quad \xi = 0, \quad \text{at} \quad z = 0 \tag{20a}$$

$$w = \mu_f \frac{\partial^2 w}{\partial z^2} + \sigma_T \nabla_h^2 T = 0, k_t \frac{\partial T}{\partial z} = h_t T, \frac{\partial \xi}{\partial z} = 0 \quad \text{at} \quad z = d \tag{20b}$$

where h_t is the heat transfer coefficient and k_t is the effective thermal conductivity. In the case of finite electric susceptibility of the boundaries, the scalar electric potential satisfies the following boundary conditions

$$\frac{\partial \phi}{\partial z} - \frac{a}{1 + \chi_e} \phi - T = 0 \qquad \text{at} \quad z = 0$$
$$\frac{\partial \phi}{\partial z} + \frac{a}{1 + \chi_e} \phi - T = 0 \qquad \text{at} \quad z = d. \tag{20c}$$

At the lower rigid boundary $(z = 0)$, $T = 0$ and the limit $a \to \infty$ gives the condition $\phi = 0$, while at the upper free surface $(z = d)$, $T \neq 0$ and in the limit when $\chi_e \to \infty$ it is noted that $D\phi - T = 0$ which is used as a boundary condition. Thus, we have used the following boundary conditions on electric potential

$$\phi = 0 \qquad \text{at} \quad z = 0$$
$$\frac{\partial \phi}{\partial z} - T = 0 \qquad \text{at} \quad z = d. \tag{20d}$$

The normal mode solution is assumed in the form

$$[w, T, \phi, \xi] = [W(z), \Theta(z), \Phi(z), Y(z)] \exp[i(a_x x + a_y y) + \omega t], \tag{21}$$

where, a_x and a_y are the wave numbers in the x and y directions, respectively, ω (real or complex) is the growth term, while W, Θ, Φ and ξ are the perturbed velocity field, temperature, electric potential and vorticity respectively. By substituting Eq. (21) into Eqs. (16)–(19) yields

$$\left[\frac{\omega}{\varphi} - \frac{\tilde{\mu}_f}{\rho_0}(D^2 - a^2) + \frac{\mu_f}{\kappa\rho_0}\right](D^2 - a^2)W = -\alpha g a^2 \Theta - \frac{2\Omega}{\varphi}\frac{\partial Y}{\partial z} + \varepsilon_0 E_0 \eta f(z)\left[a^2(D\Phi) + E_0 \eta a^2 \Theta\right] \tag{22}$$

$$[A\omega - \kappa(D^2 - a^2)]\Theta = f(z)W \tag{23}$$

$$(D^2 - a^2)\Phi = -\eta E_0 D\Theta \tag{24}$$

$$\left[\frac{\omega}{\varphi} - \frac{\tilde{\mu}}{\rho_0}(D^2 - a^2) + \frac{\mu}{\kappa\rho_0}\right]Y = \frac{2\Omega}{\varphi}DW. \tag{25}$$

Here, D stands for d/dz and $a = \sqrt{a_x^2 + a_y^2}$ is the overall horizontal wave number. In order to carry out the analysis, it is expedient to non-dimensionalize the equations as follows (an asterisk '$*$' denotes a dimensionless quantity):

$$(x, y, z) = d(x*, y*, z*), \quad W = (\kappa/d)W*, \quad \Theta = (\Delta T)\Theta*, \quad \Phi = (\eta E_0 \Delta T d)\Phi*,$$
$$\omega = (\kappa/d^2)\omega*, \quad f(z) = (\Delta T/d)f(z)*, \quad Y = (\kappa/d^2)Y*. \tag{26}$$

Substituting Eq. (26) into Eqs. (22)–(25) and dropping the asterisks for simplicity, we obtain

$$\left[\Lambda(D^2 - a^2) - 1/Da - \omega \Pr\right](D^2 - a^2)W - a^2 R_t \Theta$$
$$- \sqrt{Ta}\, DY - a^2 R_e f(z)(\Theta + D\Phi) = 0 \tag{27}$$

$$[D^2 - a^2 - \omega]\Theta + f(z)W = 0 \tag{28}$$

$$(D^2 - a^2)\Phi + D\Theta = 0 \tag{29}$$

$$\left[\Lambda(D^2 - a^2) - 1/Da - \omega \Pr\right]Y + \sqrt{Ta}\, DW = 0. \tag{30}$$

Here, $R_t = \alpha g \Delta T d^3 / \nu \kappa$ is the thermal Rayleigh number, $R_e = \eta^2 \varepsilon_0 E_0^2 (\Delta T)^2 d^2 / \mu\kappa$ the electric Rayleigh number, $\Lambda = \tilde{\mu}_f / \mu_f$ the viscosity ratio, $Da = k_1/d^2$ the Darcy number, $\Pr = \nu/\varphi\kappa$ the Prandtl number and $Ta = 4\Omega^2 d^4/\nu^2$ the Taylor number. The non-dimensional temperature gradient is taken as

$$f(z) = a_1 + 2a_2(z - 1) + 3a_3(z - 1)^2.$$

where a_1, a_2 and a_3 are constants chosen as in Table 1 such that $\int_0^1 f(z)\, dz = 1$. For the case of $a_1 = 1$, $a_2 = 0$

Table 1 Reference steady-state temperature gradients

Model	Reference steady-state temperature gradient	$f(z)$	a_1	a_2	a_3
1	Linear	1	1	0	0
2	Cubic 1	$3(z-1)^2$	0	0	1
3	Cubic 2	$0.66 + 1.02(z-1)^2$	0.66	0	0.34

and $a_3 = 0$, we recover the classical linear basic state temperature distribution (see Table 1).

The boundary conditions now become

$$W = DW = 0,\ \Theta = 0,\ \Phi = 0,\ Y = 0 \text{ at } z = 0 \qquad (31a)$$

$$W = \Lambda D^2 W + a^2 Ma\Theta = 0,\ D\Theta + Bi\Theta = 0,\ D\Phi - \Theta = 0,\ DY = 0 \text{ at } z = 1 \qquad (31b)$$

where $Bi = h_t d/k_t$ is the Biot number and $Ma = \sigma_T \Delta T d/\mu_f \kappa$ is the Marangoni number. The condition $Bi = 0$ corresponds to the case of constant heat flux or adiabatic boundary condition, while $Bi \to \infty$ corresponds to the case of isothermal boundary condition.

4 Method of solution

Equations (27)–(30) constitute an eigenvalue problem and solved using the Galerkin method (Finlayson [44]). Accordingly, the unknown variables are expanded as follows:

$$W = \sum_{m=1}^{N} A_m W_m(z),\ \Theta = \sum_{m=1}^{N} B_m \Theta_m(z),\ \Phi \sum_{m=1}^{N} C_m \Phi_m,\ Y = \sum_{m=1}^{N} D_m Y_m(z), \qquad (32)$$

where $A_m,\ B_m,\ C_m,\ D_m$ are constants, and $W_m, \Theta_m,\ \Phi_m,\ \xi_m$ are trial (basis) functions and they are assumed in the following form

$$W_m = \left(z^{m+1} - z^{m+2}\right)T_m^*,\ \Theta_m = \left(2z^m - z^{m+1}\right)T_m^*,\ \Phi_m = Y_m = (3z^{m+1} - 2z^{m+2})T_m^*, \qquad (33)$$

where $T_1^*,\ T_2^*,\ \ldots\ldots T_m^*$ are modified Chebyshev polynomials of second kind. The trial functions are chosen satisfying the respective boundary conditions except $\Lambda D^2 W + a^2 Ma\Theta = 0,\ D\Theta + Bi\Theta = 0$ and $D\Phi - \Theta = 0$ at $z = 1$ but the residual from these conditions are included as a residual from Eqs. (27)–(30). Substituting Eq. (32) into Eqs. (27)–(30), multiplying resulting Eqs. (27), (28), (29) and (30), respectively by $W_n(z), \Theta_n(z), \Phi_n(z)$ and $Y_n(z)$, and integrating from $z = 0$ to $z = 1$ and thereby with the help of Eqs. (31a, b), the following equations are obtained:

$$\begin{bmatrix} E_{nm} & F_{nm} & G_{nm} & H_{nm} \\ I_{nm} & J_{nm} & 0 & 0 \\ 0 & K_{nm} & L_{nm} & 0 \\ P_{nm} & 0 & 0 & Q_{nm} \end{bmatrix} \begin{bmatrix} A_n \\ B_n \\ C_n \\ D_n \end{bmatrix} = \begin{bmatrix} 0 \\ 0 \\ 0 \\ 0 \end{bmatrix} \qquad (34)$$

where

$$E_{nm} = \int\limits_0^1 \left\{ \Lambda\left[D^2W_nD^2W_m + 2a^2DW_nDW_m + a^4W_nW_m\right] + (Da^{-1} + \omega \overset{-1}{\text{Pr}})[DW_nDW_m + a^2W_nW_m] \right\} dz,$$

$$F_{nm} = -a^2 \int\limits_0^1 [R_t + R_e f(z)]W_n\Theta_m\, dz + a^2MaDW_n(1)\Theta_m(1),$$

$$G_{nm} = -a^2R_e \int\limits_0^1 f(z)W_nD\Phi_m dz,$$

$$H_{nm} = -\sqrt{Ta} \int\limits_0^1 W_nDY_m\, dz,$$

$$I_{nm} = -\int\limits_0^1 f(z)\,\Theta_nW_m\, dz,$$

$$J_{nm} = \int\limits_0^1 \left\{ D\Theta_nD\Theta_m + (a^2 + \omega)\,\Theta_n\Theta_m \right\} dz + Bi\,\Theta_n(1)\Theta_m(1),$$

$$K_{nm} = -\int\limits_0^1 D\Theta_m\Phi_n\, dz,$$

$$L_{nm} = -\frac{1}{4} + \int\limits_0^1 \left\{ D\Phi_nD\Phi_m + a^2\Phi_n\Phi_m \right\} dz,$$

$$P_{nm} = -\sqrt{Ta} \int\limits_0^1 Y_nDW_m\, dz,$$

$$Q_{nm} = \Lambda \int\limits_0^1 \left\{ DY_nDY_m + a^2Y_nY_m \right\} + \int\limits_0^1 \left(Da^{-1} + \omega \overset{-1}{\text{Pr}} \right)Y_nY_m dz.$$

Equation (34) has the determinant of coefficient matrix, vanishes resulting in a non-trivial solution. That is,

$$\begin{vmatrix} E_{nm} & F_{nm} & G_{nm} & H_{nm} \\ I_{nm} & J_{nm} & 0 & 0 \\ 0 & K_{nm} & L_{nm} & 0 \\ P_{nm} & 0 & 0 & Q_{nm} \end{vmatrix} = 0. \tag{35}$$

The eigenvalues are extracted from Eq. (35) for $m = n = 1$ which gives the characteristic equation:

$$Ma = \frac{4(15\eta_3 + 2\omega)}{a^2 15\langle\Theta f(z)W\rangle}\left[(\eta_1 + \omega \overset{-1}{\text{Pr}}\eta_2) + \frac{7Ta}{20(315\eta_5 + 13\omega\,\text{Pr}^{-1})} \right] - \frac{a^2R_t}{30} - a^2R_{ea}\left[\langle\Theta f(z)W\rangle + \frac{\langle Wf(z)D\Phi\rangle}{20\eta_4} \right] \tag{36}$$

where

$$\eta_1 = \Lambda\left(4 + \frac{a^4}{105} + \frac{4a^2}{15}\right) + Da^{-1}\left(\frac{2}{15} + \frac{a^2}{105}\right),$$

$$\eta_2 = \frac{2}{15} + \frac{a^2}{105},$$

$$\eta_3 = \frac{2a^2}{15} + \frac{1}{3} + \frac{Bi}{4},$$

$$\eta_4 = -\frac{1}{4} + \frac{2}{15} + \frac{13\,a^2}{315},$$

$$\eta_5 = \Lambda\left(\frac{13a^2}{315} + \frac{2}{15}\right) + Da^{-1}\frac{13}{315},$$

$$\langle\cdots\rangle = \int_0^1 (\cdots)\,dz.$$

To study the stability of the system, we take $\omega = i\omega_i$ in Eq. (36) and clear the complex quantities from the denominator which yields

$$Ma = \frac{4}{a^2 15\langle\Theta f(z)W\rangle}\left[\frac{\left(15\eta_1\eta_3\,\mathrm{Pr} - 2\omega_i^2\eta_2\right)}{\mathrm{Pr}} + \frac{7Ta\,\mathrm{Pr}\left(4725\eta_3\eta_5\,\mathrm{Pr} + 26\omega_i^2\right)}{20\left\{99225\,\eta_5^2\,\mathrm{Pr}^2 + 169\omega_i^2\right\}}\right] - \frac{4R_t}{30}$$
$$- 4R_{ea}\langle\Theta f(z)W\rangle - \frac{R_{ea}\langle Wf(z)D\Phi\rangle}{5\eta_4} + i\omega_i\Delta \tag{37}$$

where

$$\Delta = \frac{4}{a^2 15\langle\Theta f(z)W\rangle}\left[\frac{(15\eta_2\eta_3 + 2\eta_1\,\mathrm{Pr})}{\mathrm{Pr}} + \frac{7Ta\,\mathrm{Pr}(630\,\mathrm{Pr}\,\eta_5 - 195\eta_3)}{20\left\{99225\,\eta_5^2\,\mathrm{Pr}^2 + 169\omega_i^2\right\}}\right]. \tag{38}$$

Since Ma being the physical quantity it must be real. Hence, from Eq. (37) it implies $\omega_i = 0$ or $\Delta = 0\,(\omega_i \neq 0)$ and 'accordingly the condition for the steady onset ($\omega_i = 0$) is obtained. The steady onset occurs at $Ma = Ma^s$, where

$$Ma^s = \frac{4}{a^2 15\langle\Theta f(z)W\rangle}\left[15\eta_1\eta_3 + \frac{Ta\,(4725\eta_3\eta_5)}{283500\,\eta_5^2}\right]$$
$$- \frac{4R_t}{30} - 4R_{ea}\left[\langle\Theta f(z)W\rangle + \frac{\langle Wf(z)D\Phi\rangle}{20\eta_4}\right]. \tag{39}$$

The condition $\Delta = 0$ gives an expression for ω_i^2 in the form

$$\omega_i^2 = -\frac{(99225\eta_2^2\,\mathrm{Pr})^2}{169} + \frac{7Ta\,\mathrm{Pr}^2}{260\eta_2}\left[\frac{1 - 2\beta_1\,\mathrm{Pr}}{1 + 2\beta_2\,\mathrm{Pr}}\right] \tag{40}$$

where $\beta_1 = \frac{21\eta_5}{13\eta_3}$ and $\beta_2 = \frac{\eta_1}{15\eta_2\eta_3}$.

Substituting the value of ω_i^2 from Eq. (40) into Eq. (38) by noting $\Delta = 0$ yields the condition for the onset of oscillatory convection to occur at $Ma = Ma^0$, where

$$Ma^0 = \frac{4(\alpha_2\alpha_4 + \alpha_3\alpha_4^2 + \alpha_1)}{a^2 15\alpha_4\langle\Theta f(z)W\rangle} - \frac{4R_t}{30} - 4R_{ea}\langle\Theta f(z)W\rangle$$
$$- \frac{R_{ea}\langle Wf(z)D\Phi\rangle}{5\eta_4} \tag{41}$$

with

$$\alpha_1 = 4725\eta_3\eta_5 - \frac{2579850\,\mathrm{Pr}}{169},$$

$$\alpha_2 = \left[15\eta_1\eta_3 + \frac{198450\eta_2\,\mathrm{Pr}}{169}\right] + \frac{7Ta\,\mathrm{Pr}}{130},$$

$$\alpha_3 = -\frac{7Ta\eta_2\,\mathrm{Pr}}{(1690)} \text{ and}$$

$$\alpha_4 = \frac{195\eta_3 - 630\eta_5\,\mathrm{Pr}}{15\eta_2\eta_3 + 2\eta_1\,\mathrm{Pr}}.$$

Imposing the condition $\omega_i^2 > 0$, we note that

$$\mathrm{Pr} < \frac{13}{2}\left[\frac{2a^2 + 5 + 3.75Bi}{13a^2 + 42 + 13\sigma^2}\right] \text{ and } Ta > \frac{283500\eta_2\eta_5^2}{13}\left[\frac{1 + 2\beta_2\,\mathrm{Pr}}{1 - 2\beta_1\,\mathrm{Pr}}\right].$$

Thus it is clear that oscillatory convection is possible provided $\mathrm{Pr} < 1$ and the Taylor number Ta exceeds a threshold value as observed in the classical viscous liquids. For dielectric fluids, the value of Prandtl number is greater than unity (for example, $\mathrm{Pr} = 100$ for silicone oil [45], 10,000 for caster oil [46] and 480 for corn oil [47]. Under the circumstance, we restrict ourselves to the case of steady onset.

5 Results and discussion

The solution of the eigenvalue problem can be expressed symbolically as

$$f\left(R_t,\ R_e,\ Bi,\ Ta,\ Da^{-1},\ \Lambda,\ Ma,\ a,\ a_1,\ a_2,\ a_3\right) = 0 \tag{42}$$

where in the minimum of R_t or R_e or Ma is found with respect to the wave number 'a' for any chosen set of parametric values. The critical values (Ma_c, a_c) for $R_t = 0$ (absence of buoyancy force) and (R_{tc}, a_c) for $Ma = 0$ (absence of surface tension force) computed numerically are in line with those published previously. Our values of Ma_c and the corresponding a_c obtained for different Ta when $R_e = Da^{-1} = 0$, $\Lambda = f(z) = 1$ and $Bi = 10^3$ compare very well with those of Pradhan [48] (see Table 2). The obtained R_{tc} and a_c values for different Da when $R_e = Ma = Ta = 0$, $\Lambda = 1$ and $f(z) = 1$ for isothermal-lower rigid and insulated-upper surface are compared in Table 3 with those of Lebon and Cloot [49] and an excellent agreement is found. The results of Char and Chiang [37] are exhibited along with our obtained results in Fig. 2 for lower rigid-isothermal and upper free-insulated to temperature perturbations when $Ta = Da^{-1} = 0$, $\Lambda = 1$ and $Ma = 0$ for $f(z) = 1$. It is seen that the results complement each other showing the accuracy of the numerical computation.

Figure 3a, b give the variation of Ma_c and R_{tc} with Bi for the case of cubic 1, cubic 2 and linear temperature profiles when $\Lambda = 1$, $Ta = 10$ and $Da^{-1} = 0$. For the case of $Bi = 0$, an insulated surface retains more energy within the porous layer and thus the system is less stable. However, increase in Bi is to increase R_{tc} and Ma_c indicating their effect is to delay electro-thermal convection (ETC). This may be credited that an increase in Bi leads thermal disturbances to dissipate easily into the ambient surroundings due to a better convective heat transfer co-efficient at the top surface and thus higher heating is required to make the system unstable. It is also apparent that the dielectric fluid-saturated porous layer under an AC vertical electric field becomes more stable with an increase in Bi.

Figure 4 shows the values of R_{tc} ($Ma = 0$) and Ma_c ($R_t = 0$) as a function of Taylor number Ta for different

Table 3 Comparison of R_{tc} and a_c for different values of Da when $R_e = Bi = Ma = Ta = 0$ and $\Lambda = 1$

Da	Lebon and Cloot [46]		Present study	
	R_{tc}	a_c	R_{tc}	a_c
10^{-9}	27.3	2.30	27.34	2.33
10^{-6}	27.3	2.29	27.34	2.33
10^{-3}	28.5	2.28	28.47	2.34
∞	669	2.08	669.0	2.08

values of R_e when $\Lambda = 1$, $Bi = 2$, $Da^{-1} = 0$ and different forms of $f(z)$. It is found that R_{tc} and Ma_c increase with increasing Ta. Thus the Coriolis force has a stabilizing effect on the system for different forms of basic temperature gradients. The system is found to be more stable for cubic1 temperature gradient when compared to cubic2 and least stable for a linear temperature profile.

Figure 5 shows R_{tc} and Ma_c against Da^{-1} when $Bi = 2$, $\Lambda = 1$ and $Ta = 10$. Increase in Da^{-1} results in the decrease of permeability of the porous medium which in turn hinders the fluid flow in porous media and hence higher values of R_{tc} are required for the onset of ETC. Figure 6 shows R_{tc} and Ma_c versus Λ for $Bi = 2$, $Da^{-1} = 0$ and $Ta = 10$. Increase in the value of Λ amounts to increase in the viscous diffusion which retards the fluid flow resulting in higher heating requirement for the onset of ETC. Moreover, from Figs. 3, 4, 5 and 6 it is evident that increase in R_e leads to decrease in Ma_c and R_{tc}, in general. That is, higher the strength of the electric field is to hasten the onset due to an increase in the destabilizing electrostatic energy to the system. In other words, the presence of electric field facilitates the transfer of heat more effectively and hence accelerates' ETC at a lower value of Ma_c or R_{tc}. This result is

Table 2 Comparison of Ma_c, R_{tc} and a_c for different values of Ta when $Da^{-1} = R_e = 0$, $\Lambda = 1$ and $Bi = 1000$

Ta	Pradhan [48]				Present Study			
	$R_t = 0$		$Ma = 0$		$R_t = 0$		$Ma = 0$	
	a_c	Ma_c / Bi	a_c	R_{tc}	a_c	Ma_c / Bi	a_c	R_{tc}
0.0	3.01	32.073	2.68	1101.1	3.01	32.170	2.68	1099.12
6.25	3.03	32.227	2.68	1108.5	3.03	32.317	2.69	1106.2
31.25	3.09	32.795	2.70	1136.4	3.08	32.888	2.74	1133.87
62.50	3.16	33.467	2.79	1169.4	3.15	33.565	2.79	1167.16
187.5	3.36	35.835	2.972	1291.5	3.38	35.950	2.97	1289.19
625.0	3.96	41.829	3.39	1638.0	3.95	41.987	3.39	1635.64
1875.0	4.87	51.795	4.0	2357.2	4.86	52.037	4.01	2356.34
6250.0	6.35	68.348	4.926	4046.5	6.33	68.761	4.93	4042.54
18,750.0	8.22	89.38	6.0	7225.6	8.20	90.055	5.99	7223.81
62,500.0	11.02	120.67	7.422	14,513.7	10.99	121.810	7.41	14,504.5
187,500.0	14.46	159.11	9.0	28,392.0	14.42	160.01	8.98	28,391.0
625,000.0	17.27	220.69	11.06	60,746.8	19.46	220.051	11.07	60,745.91
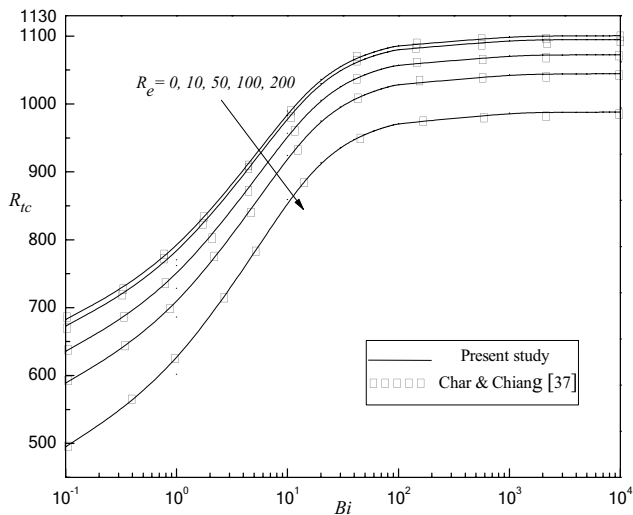
Fig. 2 Comparison of R_{tc} as a function of Bi for different values of R_e for $Da^{-1} = Ta = 0$ and $\Lambda = 1$
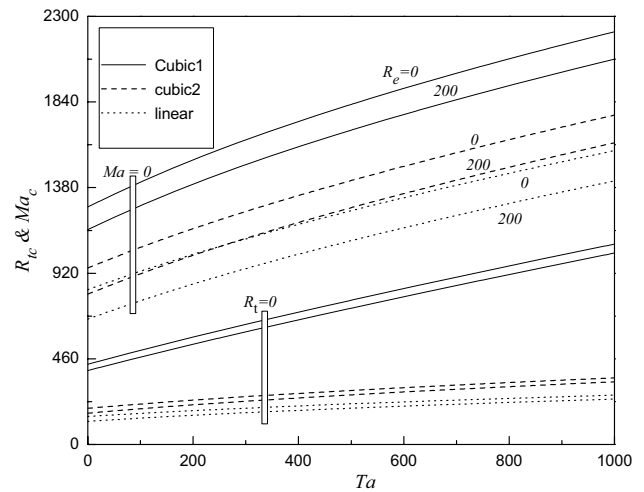

Fig. 4 Variation of R_{tc} and M_{ac} verses Ta for different values of R_e and for $\Lambda = 1$, $Bi = 2$ and $Da^{-1} = 0$

true for all the types of temperature profiles considered. That is, for different values of R_e, it is found that

$$\left(Ma_c\right)_{linear < cubic2 < cubic1} < \left(R_{tc}\right)_{linear < cubic2 < cubic1}.$$

The locus of R_{ec} and M_{ac} for different Ta when $\Lambda = 1$, $Da^{-1} = 25$, $R_t = 25$ and $Bi = 2$ is shown in Fig. 7. For all types of temperature gradients considered, it is found that R_{ec} and Ma_c increase as Ta increases and hence rotation has a stabilizing effect on the system. Thus, when the electric force is predominant then the gravitational force

becomes negligible. This is true for all the temperature gradients. The presence of electric field is to facilitate the heat transfer more effectively and hence hastens the onset of Bénard–Marangoni ETC. The system is found to be more stable for cubic 1 temperature gradient when compared to cubic 2 type of temperature gradient, and the least stable for the linear temperature gradient. That is,

$$(Ma_c \text{ or } R_{ec})_{\text{linear}} < (Ma_c \text{ or } R_{ec})_{\text{cubic 2}} < (Ma_c \text{ or } R_{ec})_{\text{cubic 1}}$$
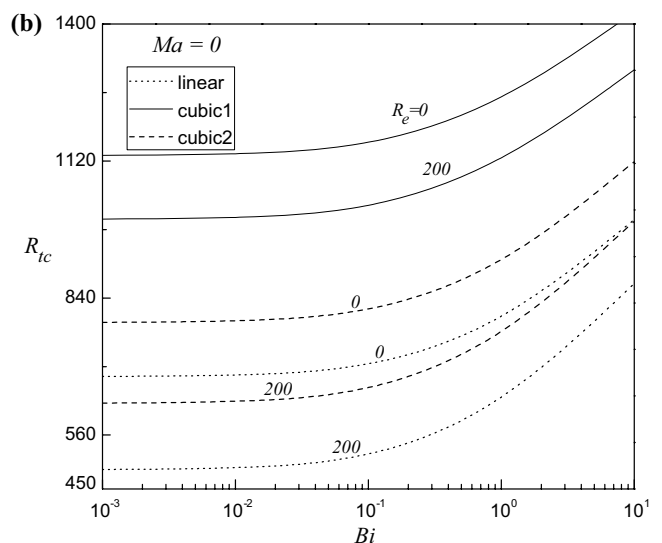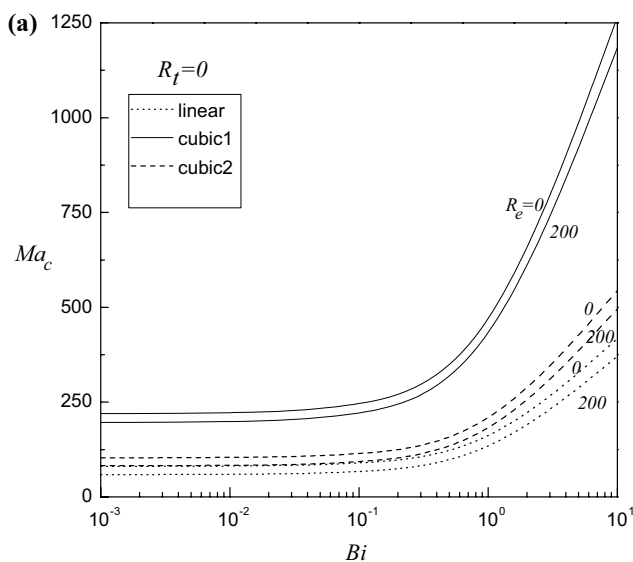

Fig. 3 Variation of (**a**) M_{ac} and (**b**) R_{tc} verses Bi for different values of R_e and for $\Lambda = 1$, $Ta = 10$ and $Da^{-1} = 0$
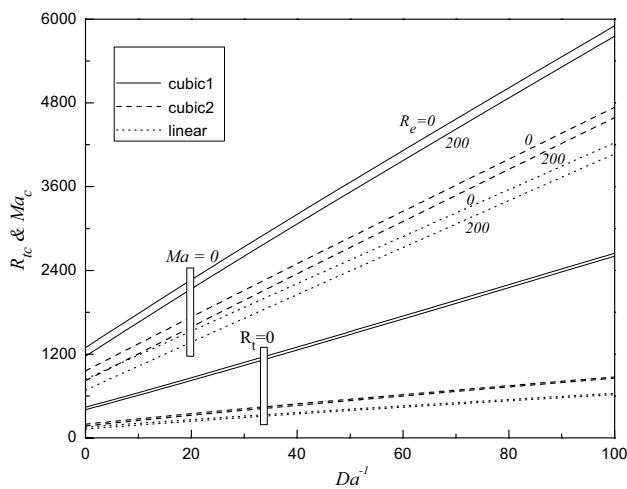
Fig. 5 Variation of R_{tc} and M_{ac} verses Da^{-1} for different values of R_e and for $\Lambda = 1, Bi = 2$ and $Ta = 10$
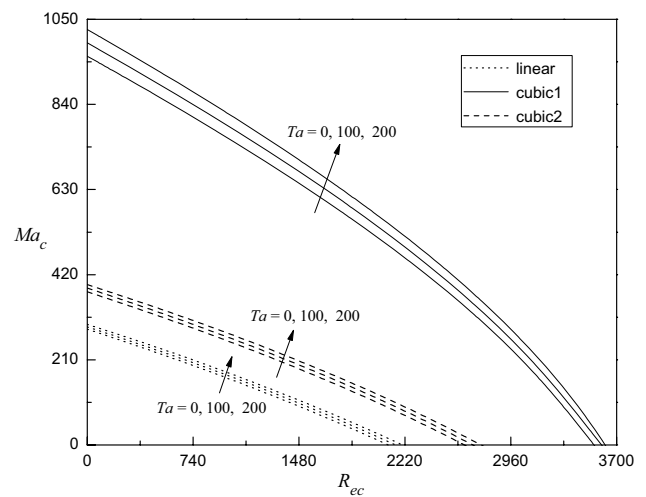

Fig. 7 Locus of M_{a_c} verses R_{ec} for different values of Ta and for $\Lambda = 1$, $Da^{-1} = 25$, $R_t = 25$ and $Bi = 2$
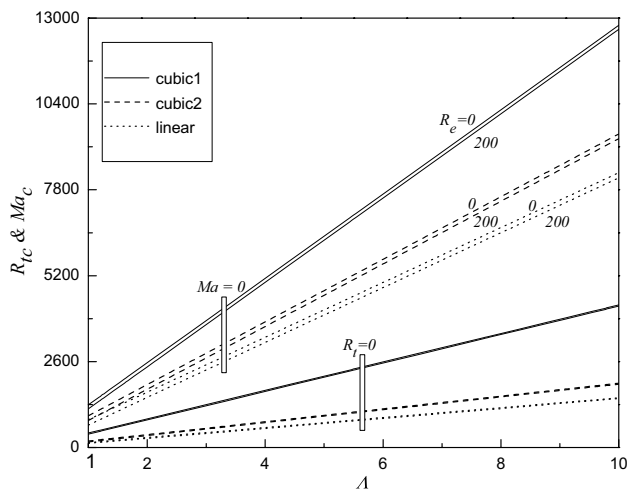
- The system is more stable with increasing Biot number Bi.
- As Taylor number increases the critical stability parameters increase indicating the Coriolis force has a stabilizing effect on the system.
- The system is more stable for temperature gradient of cubic 1 while the linear temperature gradient is the least stable. That is,

$$(R_{ec} \text{ or } M_{a_c})_{\text{linear}} < (R_{ec} \text{ or } M_{a_c})_{\text{cubic2}} < (R_{ec} \text{ or } M_{a_c})_{\text{cubic1}}.$$

- The critical electric Rayleigh number R_{ec} decreases with an increase in the Marangoni number Ma.

Fig. 6 Variation of R_{tc} and M_{ac} verses Λ for different values of R_e and for $Da^{-1} = 0$, $Bi = 2$ and $Ta = 10$

Compliance with ethical standards

Conflict of interest The authors declare that they have no conflict of interest.

6 Conclusions

The aforesaid findings give an outline to the entire exploration for the effect of coupling of buoyancy, surface tension, electric, viscous, Coriolis forces and the effect of permeability on the onset of ETC in a liquid-saturated layer of porous medium. The principle of exchange of stability is found to be valid and the problem of eigenvalue is solved using the Galerkin method for different basic temperature gradients. The results may be summarized as follows:

- Increase in the Darcy number is to speed up the onset of Bénard- Marangoni ETC while the adverse trend is observed with increasing ratio of viscosities.

References

1. Thoma AM, Morari M (2006) Control of fluid flow. Springer, Berlin
2. Melcher JR, Schwarz WJ (1968) Interfacial relaxation overstability in a tangential electric field. Phys Fluids 11:2604–2616. https://doi.org/10.1063/1.1691866
3. Melcher JR, Smith CV (1969) Electrohydrpdynamic charge relaxation and interfacial perpendicular-field instability. AIP Phys Fluids 12:778. https://doi.org/10.1063/1.1692556
4. Larsen JNE, Ran H, Zhang Y (2009) Electrohydrodynamic cooled laptop, Semiconductor thermal measurement and management symposium. 25th Annual IEEE semiconductor thermal measurement and management symposium. https://doi.org/10.1109/stherm.2009.4810773

5. Tassavur S (2011) Super Cool 'EHD Pump' by NASA cools devices in Space. http://onlygizmos.com/super-cool-ehd-pump-by-nasa-cools-devices-in-space/2001/05

6. Taylor GI (1966) Studies in electrohydrodynamics, circulation produced in a drop by an electric field. Proc R Soc Lond A 291:159–166. https://doi.org/10.1098/rspa.1966.0086

7. Turnbull RJ, Melcher JR (1969) Electrodynamic Rayleigh–Taylor bulk instability. Phys Fluids 12:1160–1166. https://doi.org/10.1063/1.3435342

8. Roberts PH (1969) Electrohydrodynamic convection. Q J Mech Appl Math 22:211–220. https://doi.org/10.1093/qjmam/22.2.211

9. Turnbull RJ (1969) Effect of dielectrophoretic forces on the Bénard instability. Phys Fluids 12:1809–1815. https://doi.org/10.1063/1.1692745

10. Takashima M (1976) The effect of rotation on electrohydrodynamic instability. Can J Phys 54:342–347. https://doi.org/10.1139/p76-039

11. Jones TB (1979) Electrohydrodynamically enhanced heat transfer in liquids—A review. Adv Heat Transf 14:107–148. https://doi.org/10.1016/S0065-2717(08)70086-8

12. Castellanos A (1991) Coulomb-driven convection in electrohydrodynamics. IEEE Trans Elect Insul 26(6):1201–12015. https://doi.org/10.1109/14.108160

13. Stiles PJ (1991) Electro-thermal convection in dielectric liquids. Chem Phys Lett 179(3):311–315. https://doi.org/10.1016/0009-2614(91)87043-B

14. Pontiga F, Castellanos A (1993) Physical mechanisms of instability in aliquid layer subjected to an electric field and a thermal gradient. Phys Fluids 6(5):1684–1701. https://doi.org/10.1063/1.868231

15. Chang JS, Watson A (1994) Electromagnetic hydrodynamics. IEEE Trans Dielectr Electr Insul 1:871–895

16. Moreno RZ, Bonet EJ, Trevisan OV (1996) Electric alternating current effects on flow of oil and water in porous media. In: Vafai K, Shivakumar PN (eds) Proceedings of the international conference on porous media and their applications in science. Engineering and Industry, Hawaiir, pp 147–172

17. Del Rio JA, Whitaker S (2001) Electrohydrodynamics in porous media. Transp Porous Media 440:385–405. https://doi.org/10.1023/A:1010762226382

18. Siddheshwar PG (2004) Thermorheological effect on magnetoconvection in weak electrically conducting fluids under 1 g or µg. Pramana J Phys 62:61–68

19. Othman MI (2004) Electrohydrodynamic instability of a rotating layer of a viscoelastic fluid heated from below. ZAMP 55:468–482. https://doi.org/10.1007/s00033-003-1156-2

20. Shivakumara IS, Nagashree MS, Hemalatha K (2007) Electrothermoconvective instability in a heat generating dielectric fluid layer. Int Commun Heat Mass Trans 34:1041–1047. https://doi.org/10.1016/j.icheatmasstransfer.2007.05.006

21. Rudraiah N, Gayathri MS (2009) Effect of thermal modulation on the onset of electrothermoconvection in a dielectric fluid saturated porous medium. ASME J Heat Transf 131:101009–101015. https://doi.org/10.1115/1.3180709

22. Ruo AC, Chang MH, Chen F (2010) Effect of rotation on the electrohydrodynamic instability of a fluid layer with an electrical conductivity gradient. Phys Fluids 22:024102-1–024102-11. https://doi.org/10.1063/1.3308542

23. Shivakumara IS, Chiu-On N, Nagashree MS (2011) The onset of electrothermoconvection in a rotating Brinkman porous layer. Int J Eng Sci 9:946–963. https://doi.org/10.1016/j.ijengsci.2011.02.010

24. Siddheshwar PG, Radhakrishna D (2012) Linear and nonlinear electroconvection under AC electric field. Commonlinear Sci Numer Simul 17:2883–2893. https://doi.org/10.1016/j.cnsns.2011.11.009

25. Shivakumara IS, Akkanagamma M, Chiu-On N (2013) Electrohydrodynamic instability of a rotating couple stress dielectric fluid layer. Int J Heat Mass Trans 62:761–771. https://doi.org/10.5958/2321-581X.2015.00009.4

26. Wu J, Traore P (2015) A finite-volume method for electrothermoconvective phenomena in a plane layer of dielectric liquid. Numer Heat Transf A 74(5):471–500. https://doi.org/10.1080/10407782.2014.986410

27. Yadav D (2016) Electrothermal instability in a porous medium layer saturated by a dielectric nanofluid. J Appl Fluid Mech 9(5):2123–2132. https://doi.org/10.18869/acadpub.68.236.25140

28. Yadav D (2018) The influence of pulsating throughflow on the onset of electrothermoconvection in a horizontal porous medium saturated by a dielectric nanofluid. J. App. Fluid Mech 11(6):1679–1689. https://doi.org/10.18869/acadpub.73.249.29048

29. Rahma G, Hassem W, Perez AT, Naceur M (2019) Numerical study of electroconvection and electrothermoconvection in solar chimneygeometry. Eur J Electr Eng 21(2):171–179. https://doi.org/10.18280/ejee.210207

30. Wu J, Traore P, Zhang M, Perez AT, Vazquez PA (2016) Charge injection enhanced natural convection heat transfer in horizontal concentric annuli filled with a dielectric liquid. Int J Heat Mass Trans 92:139–148. https://doi.org/10.1016/j.ijheatmasstransfer.2015.08.088

31. Luo K, Wu J, Yi Hong-Liang, Tan He-Ping (2016) Lattice Boltzmann model for Coulomb-driven flows in dielectric liquids. Phys Rev E 93:023309. https://doi.org/10.1103/PhysRevE.93.023309

32. Shivakumara IS, Lee Jinho, Vejravelu K, Akkanagamma M (2012) Electrothermal convection in a rotating dielectric fluid layer: effect of velocity and temperature boundary conditions. Int Heat Mass Trans 55:2984–2991. https://doi.org/10.1016/j.ijheatmasstransfer.2012.02.010

33. Ashwini R, Nanjundappa CE, Shivakumara IS (2019) Penetrative electrothermal-convection in a dielectric fluid saturated porous layer via internal heating: effect of Boundary conditions. Int J Appl Comput Math 5:1–17. https://doi.org/10.1007/s40819-019-0619-x

34. Nield DA, Bejan A (2017) Convection in porous media, Sixteenth edn. Springer-Verlag, New York. https://doi.org/10.1007/978-1-4614-5541-7

35. Koschmieder EL, Prahl SA (1990) Surface-tension-driven Bénard convection in small containers. J Fluid Mech 215:571–583. https://doi.org/10.1017/S0022112090002762

36. Pasquetti R, Cerisier P, Le Niliot C (1994) Laboratory and numerical investigations on cylindrical Bénard–Marangoni convection. Phys Fluids 14:277–288. https://doi.org/10.1063/1.1424307

37. Char MI, Chiang KT (1994) Boundary effects on the Bénard-Marangoni instability under an electric field. Appl Sci Res 52:331–354. https://doi.org/10.1007/BF00936836

38. Douiebe A, Hannoui M, Lebon G, Benaboud A, Khmou A (2001) Effects of AC electric field and rotation on Bénard–Marangoni convection. Flow Turbul Comb 67:185–204. https://doi.org/10.1023/A:1015038222023

39. Hennenberg M, Saghir MZ, Rednikov A, Legros JC (1997) Porous media and the Bénard–Marangoni problem. Trans Porous Media 27:327–355. https://doi.org/10.1023/A:1006564129233

40. Rudraiah N (2007) Effect of combined brinkman-electric boundary layer on the onset of marangoni electroconvection in a poorly conducting fluid-saturated porous layer cooled from below in the presence of an electric field. J Porous Media 10(5):421–434. https://doi.org/10.1615/JPorMedia.v10.i5.10

41. Nield DA (1975) The onset of transient convective instability. J Fluid Mech 71:441–454. https://doi.org/10.1017/S0022112075002662

42. Chandrasekhar S (1961) Hydrodynamics and hydromagnetic stability. Oxford University, Claredon Press, London

43. Maekawa T, Abe K, Tanasawa I (1992) Onset of natural convection under an electric field. Int J Heat Mass Trans 35:613–621. https://doi.org/10.1016/0017-9310(92)90120-H

44. Finlayson BA (1972) Method of weighted residuals and variational principles. Academic Press, New York

45. Rahal S, Ceriser P, Azuma H (2007) Benard-Marangoni convection in a small circular container: influence of the Biot and Prandtl numbers on pattern dynamics and free surface deformation. Exp Fluids 43:547–554. https://doi.org/10.1007/s00348-007-0323-1

46. Davis JT (1972) Turbulence phenomena: an introduction to the eddy transfer of momentum, mass and heat particularly at interfaces. Academic Press, New York

47. Martin PJ, Richardson AT (1984) Conductivity models of electrothermal convection in a plane layer of dielectric liquid. J Heat Transf 106(1):131–136. https://doi.org/10.1115/1.3246625

48. Pradhan GK (1972) Buoyancy-surface tension instability in a rotating fluid layer. Indian J Pure Appl Math 4:215–225

49. Lebon G, Cloot A (1986) Thermodynamical modelling of fluid flows through porous media: application to natural convection. Int J Heat Mass Trans 29:381–390. https://doi.org/10.1016/0017-9310(86)90208-5